Journal of Nuclear Medicine, published on September 30, 2021 as doi:10.2967/jnumed.121.262790

The Added Value of ^{68}Ga-FAPI-PET/CT in Patients with Head and Neck Cancer of Unknown Primary with ^{18}F-FDG Negative Findings

Bingxin Gu [1], Xiaoping Xu [1], Ji Zhang [1], Xiaomin Ou [2], Zuguang Xia [3], Qing Guan [4], Silong Hu [1], Zhongyi Yang [1] and Shaoli Song [1]

[1] Department of Nuclear Medicine, Fudan University Shanghai Cancer Center; Department of Oncology, Shanghai Medical College, Fudan University; Center for Biomedical Imaging, Fudan University; Shanghai Engineering Research Center of Molecular Imaging Probes; Department of [2] Radiation Oncology, [3] Medical Oncology, and [4] Head and Neck Surgery, Fudan University Shanghai Cancer Center; Shanghai, PR China

First author:

Bingxin Gu, MD, gubingxin5117@163.com

Correspondence to:

Shaoli Song, MD, shaoli-song@163.com; Zhongyi Yang, MD, yangzhongyi21@163.com

Address: No. 270, Dong'an Road, Xuhui District, Shanghai 200032, PR China

Tel: +86-18121299622

Funding information This work was funded by National Natural Science Foundation of China (Grant number 81771861, 81971648, and 81901778) and Shanghai Anticancer Association Program (Grant number HYXH2021004).

Running title: ^{68}Ga-FAPI-PET/CT in HNCUP

Word Count: 4968

ABSTRACT

^{18}F-fluorodeoxyglucose (^{18}F-FDG) positron emission tomography/computed tomography (PET/CT) plays an important role in locating of primary tumor for patients with head and neck cancer of unknown primary (HNCUP). Nevertheless, it can be challenging to locate the primary malignancy in ^{18}F-FDG-PET/CT scan in some cases. As ^{68}Ga-radiolabeled fibroblast activation protein inhibitor (FAPI) PET/CT has promising results in detecting different tumor entities, our study aimed to evaluate the performance of ^{68}Ga-FAPI-PET/CT for detecting the primary tumor in HNCUP patients with negative ^{18}F-FDG findings.

Methods: A total of eighteen patients (16 males and 2 females; median age, 55 years; range, 24-72 years) with negative ^{18}F-FDG findings were enrolled in this study. All patients underwent ^{18}F-FDG and ^{68}Ga-FAPI-PET/CT within one week. Biopsy and histopathological examinations were done in the sites with positive ^{68}Ga-FAPI-PET/CT findings.

Results: ^{68}Ga-FAPI-PET/CT detected the primary tumor in 7 out of 18 patients (38.89%). Among the 7 patients, in respect of the primary tumor sites, 1 was in nasopharynx, 2 were in palatine tonsil, 2 were in submandibular gland, and 2 were in hypopharynx. The primary tumors showed moderate to intensive uptake of FAPI (mean SUV_{max}, 8.79; range, 2.60-16.50) and excellent tumor-to-contralateral normal tissue ratio (mean SUV_{max} ratio, 4.50; range, 2.17-8.21). In lesion-based analysis, a total of 65 lymph nodes and 17 bone metastatic lesions were identified. The mean SUV_{max} of lymph node metastases were 9.05 ± 5.29 for FDG and 9.08 ± 4.69 for FAPI (p = 0.975); as for bone metastases, the mean SUV_{max} were 8.11 ± 3.00 for FDG and 6.96 ± 5.87 for FAPI, respectively (p = 0.478). The mean tumor-to-background ratio (TBR) values of lymph node and bone metastases were 10.65 ± 6.59 vs. 12.80 ± 8.11 (p = 0.100) and 9.08 ± 3.35 vs. 9.14 ± 8.40 (p = 0.976), respectively.

Conclusion: We presented first evidence of diagnostic role of ^{68}Ga-FAPI-PET/CT in HNCUP, and our study demonstrated that ^{68}Ga-FAPI-PET/CT had the potential to improve the detection rate of primary tumor in HNCUP patients with negative FDG findings. Moreover, ^{68}Ga-FAPI had similar performance in assessing metastases with ^{18}F-FDG.

Keywords: ^{68}Ga-FAPI; Head and neck; Cancer of unknown primary; Metastases

INTRODUCTION

Head and neck cancer of unknown primary (HNCUP) is defined as a metastatic disease in the cervical lymph nodes with an unidentifiable primary tumor (*1*), even after a thorough diagnostic workup according to the National Comprehensive Cancer Network (*2*) and American Society of Clinical Oncology guidelines (*3*). HNCUP constitutes 1-5% of all head and neck cancers (*4,5*). Squamous cell carcinoma (SCC) is the most common pathological type of HNCUP, and approximately 90% of these cases are associated with human papillomavirus (*1*). The most frequent primary site of HNCUP is oropharynx, accounting for 80-90% (*6*). However, some factors, like small tumor volume, hidden location, slow growth rate, and tumor involution, hinder primary site identification (*7*). The absence of primary tumor identification may result in uncertain treatment decisions and increasing psychological burden for patients with HNCUP (*8*).

Medical imaging plays an important role in oncology, particularly in tumor location (*9*). Conventional imaging modalities, Computed Tomography (CT) and Magnetic Resonance Imaging (MRI), can provide plentiful anatomical information about primary and metastatic malignancies. However, the detection rates of primary site for these two imaging modalities range from 9 to 23% in HNCUP (*10-12*). Positron emission tomography/computed tomography (PET/CT), a typical molecular imaging modality, outperforms CT and MRI in identifying primary tumor with a detection rate of 25-69% by using ^{18}F-fluorodeoxyglucose (^{18}F-FDG) (*13-16*). Nevertheless, some limitations hamper the application of ^{18}F-FDG-PET/CT in primary tumor identification for HNCUP (*17,18*). Firstly, physiological FDG uptake can be seen in any lymphatic structure (especially Waldeyer's ring), salivary glands, and brown fat. Secondly, symmetrical vocal cords and neck muscles uptake are commonly seen if the patient talks or coughs during the uptake period. Thirdly, infection and chronic inflammation (e.g., nasopharyngitis, amygdalitis, and gingivitis) can also result

in high FDG uptake. These limitations may lead to false positive findings with a rate of 16-25% (*4,13,16*). Last but not least, false negative FDG uptake can be seen in small, mucinous, well-differentiated, and necrotic lesions (*18*). Therefore, novel specific radiopharmaceuticals with low background uptake in head and neck, which may better improve the detection rate of primary tumor in HNCUP, are in urgent need.

Cancer associated fibroblasts (CAFs), accounting for high proportion of most solid tumor mass, plays a vital role in tumor growth, migration, and progression (*19*). The major feature to discriminate CAFs from normal fibroblasts is the overexpression of fibroblast activation protein (FAP) (*20*). The presence of FAP was observed on a variety of epithelial and mesenchymal malignancies (*21,22*). Recently, ^{68}Ga-radiolabeled fibroblast activation protein inhibitor (FAPI), a novel FAP-targeted PET tracer, has shown great value in diagnosis of diverse carcinomas (*23,24*). Furthermore, some studies (*25,26*) demonstrated that ^{68}Ga-FAPI revealed high uptake in primary tumors and low background noise of the head and neck region. These promising findings indicate ^{68}Ga-FAPI could serve as a potential alternative to ^{18}F-FDG for the assessment of head and neck cancers.

Thus, the aim of this study was to investigate the value of ^{68}Ga-FAPI-PET/CT for identifying primary tumor of FDG-negative HNCUP.

MATERIALS AND METHODS

Patient Selection

For patients whose primary tumor couldn't be identified by thorough medical history, clinical examination, medical imaging (e.g., contrast-enhanced CT, contrast-enhanced MRI, Ultrasound, and ^{18}F-FDG-PET/CT) and endoscopy, ^{68}Ga-FAPI-PET/CT was recommended to them for identifying primary tumor based on decision from

multidisciplinary team of head and neck cancer (Fig. 1A). In addition to patients with FDG reported negatively for the localization of the primary tumor, ^{68}Ga-FAPI-PET/CT was also recommended to patients with FDG reported positively for the localization of the primary tumor who underwent a biopsy which was negative. To further investigate the role of ^{68}Ga-FAPI-PET/CT in HNCUP, inclusion criteria were as follows: (i) adult patients (age > 18 and < 80 years); (ii) pathology confirmed metastatic cervical carcinoma by fine-needle aspiration; (iii) conventional imaging modalities (e.g., contrast-enhanced CT, contrast-enhanced MRI or Ultrasound) couldn't provide positive finding of primary tumor; (iv) both ^{18}F-FDG and ^{68}Ga-FAPI-PET/CT were performed. The exclusion criteria were (i) patients with lymphomas or non-head and neck original cancers, confirmed by immunohistochemistry; (ii) patients with both positive ^{18}F-FDG and ^{68}Ga-FAPI-PET/CT findings for primary tumors, including anaplastic thyroid carcinoma, lymphoepithelioma-like carcinoma, and biopsy-negative but clinically diagnosed nasopharyngeal carcinoma; (iii) patients with two or more malignant tumors history; (iv) patients unwilling to take ^{18}F-FDG or ^{68}Ga-FAPI-PET/CT. ^{18}F-FDG-PET/CT reported negatively for localization of primary tumor in patients with HNCUP would be regard as negative ^{18}F-FDG-PET/CT findings. This prospective study was approved by Fudan University Shanghai Cancer Center Institutional Review Board (ID 2004216-25) conducted in accordance with the 1964 Declaration of Helsinki and its later amendments or comparable ethical standards, and all subjects signed an informed consent form.

Radiopharmaceuticals and PET/CT Scanning Procedure

^{18}F-FDG was produced automatically using Explora FDG_4 module with cyclotron (Siemens CTI RDS Eclips ST, Knoxville, Tennessee, USA) in our center. DOTA-FAPI-04 (Jiangsu Huayi Technology CO., LTD, Jiangsu, China)

was radiolabeled with ^{68}Ga-solution (elution from the ^{68}Ge generator IGG100, Eckert & Ziegler, Berlin, Germany) according to Lindner et al (*27*). Radiochemical purity of ^{18}F-FDG and ^{68}Ga-FAPI were both over 95%.

Firstly ^{18}F-FDG-PET/CT was performed, then ^{68}Ga-FAPI-PET/CT was performed within one week. For ^{18}F-FDG PET/CT scanning, patients fasted at least 6 hours, maintaining venous blood glucose levels under 10 mmol/L prior to ^{18}F-FDG administration. But this was not necessary for ^{68}Ga-FAPI-PET/CT scanning. After injecting with 260.64 ± 40.81 MBq of ^{18}F-FDG or 143.71 ± 16.19 MBq of ^{68}Ga-FAPI, patients were kept in a quiet environment for approximately 60 mins prior to examination. All images were obtained on a Biograph mCT Flow scanner (Siemens Medical Solutions). PET image data sets were reconstructed iteratively using an ordered-subset expectation maximization iterative reconstruction by applying CT data for attenuation correction. Two experienced nuclear medicine physicians independently analyzed and interpreted the images blinded, and they reached a consensus in case of inconsistency.

Increased radioactivity of primary and metastatic lesions compared with the muscle background uptake was defined as being positive, verified by biopsy or follow-up. For quantitative analysis, maximum or mean of standardized uptake value (SUV) normalized to body weight were manually computed for primary and metastatic lesions and healthy tissues by drawing a 3-dimensional volume of interest. Meanwhile, SUV_{max} ratio for primary tumor was defined as the quotient of the SUV_{max} of primary tumor and the contralateral normal tissue, and tumor-to-background ratio (TBR) for primary and metastatic lesions was calculated according to the formula: $TBR = tSUV_{max}/bSUV_{mean}$, where $tSUV_{max}$ is the maximum SUV of tumor lesion, and $bSUV_{mean}$ is the mean SUV of muscle. The size of primary and metastatic lesions was measured by CT.

Statistical Analyses

All statistical analyses were performed using SPSS 25.0 (IBM, Armonk, NY, USA). Means with standard deviation or medians with ranges were used to describe continuous characteristics. To compare the uptake of ^{18}F-FDG and ^{68}Ga-FAPI in metastatic lesions, two-sample t tests were used. Two-tailed $p < 0.05$ were considered statistically significant.

RESULTS

Patients

A total of thirty-two patients were enrolled consecutively from our center during June 2020 to Feb 2021, and eighteen patients were included for further analysis according to the inclusion and exclusion criteria (Fig. 1B). The basic clinical characteristics were presented in Table 1. Among the included eighteen patients (16 males and 2 females; median age, 55 years; range, 24-72 years), two (11.11%) were infected with Epstein-Barr virus; six (33.33%) were infected with human papillomavirus; sixteen (88.89%) were pathologically diagnosed with cervical lymph node SCC and two (11.11%) were adenocarcinoma.

Comparison of ^{18}F-FDG and ^{68}Ga-FAPI-PET/CT in Metastatic Lesions

A total of 65 lymph node and 17 bone metastases were detected by both ^{18}F-FDG and ^{68}Ga-FAPI-PET/CT (Fig. 2, Table 2 and Supplemental Table 1). Both tracers showed intensive uptake in lymph node and bone metastases. The mean SUV_{max} value of lymph node metastases was 9.05 ± 5.29 for FDG and 9.08 ± 4.69 for FAPI ($p = 0.975$). In case of TBR, FAPI was a little higher than FDG (12.80 ± 8.11 and 10.65 ± 6.59, respectively). But the difference was not significant ($p = 0.100$). For bone metastases, the mean SUV_{max} value was 8.11 ± 3.00 for FDG and 6.96 ± 5.87 for

FAPI (p = 0.478), and the mean TBR value was 9.08 ± 3.35 and 9.14 ± 8.40 (p = 0.976), respectively. Generally, no significant uptake difference was observed between FDG and FAPI in lymph node and bone metastases, indicating that ^{68}Ga-FAPI-PET/CT had similar performance as ^{18}F-FDG-PET/CT in assessing metastases of head and neck cancers.

^{68}Ga-FAPI-PET/CT Imaging Results of Primary Tumors

Seven out of eighteen (38.89%) FDG-negative patients identified primary tumors by ^{68}Ga-FAPI-PET/CT, pathologically confirmed by subsequent biopsy. In terms of pathological type, ^{68}Ga-FAPI-PET/CT showed a higher detection rate in adenocarcinoma (2/2, 100%) than SCC (5/16, 31.25%). One of the primary sites was in nasopharynx, two were in palatine tonsil (Fig. 3), two were in submandibular gland (Fig. 4), and two were in hypopharynx (Supplemental Fig. 1 and Table 3).

According to the 8th edition American Joint Committee on Cancer TNM staging classification, the TNM stage for these seven patients ranged from I to IVC. The smallest primary tumor size detected by ^{68}Ga-FAPI-PET/CT was 5 × 3 mm. The mean SUV_{max} value of ^{68}Ga-FAPI for primary tumors was 8.79 (range, 2.60-16.50), and the mean TBR value was 11.50 (range, 2.36-27.50). When compared to the contralateral normal tissue, primary tumor showed a remarkable higher uptake of FAPI, with a mean SUV_{max} ratio of 4.50 (range, 2.17-8.21).

DISCUSSION

Identifying the primary tumor remains a concern for patients with HNCUP, though the development in imaging, endoscopy, and pathology techniques. If without any positive findings by non-invasive procedures, invasive diagnostic

operations, like tonsillectomy, are performed with a risk of bleeding or infection (*5*). Thus, novel non-invasive methods may be needed for improving detection rate of primary tumor in HNCUP patients. This study investigated the performance of ^{68}Ga-FAPI-PET/CT in identifying primary tumor of FDG-negative HNCUP. Our results demonstrated that ^{68}Ga-FAPI can dramatically improve the detection rate of primary tumor in HNCUP patients comparing to ^{18}F-FDG. Furthermore, ^{68}Ga-FAPI may show similar performance with ^{18}F-FDG in assessing metastases.

The current study exhibited a 38.89% (7/18) detection rate of primary tumor by ^{68}Ga-FAPI-PET/CT. Notably, these patients were all with false negative ^{18}F-FDG-PET/CT findings. The sites of false negative ^{18}F-FDG-PET/CT findings in this study were nasopharynx, palatine tonsil, submandibular gland, and hypopharynx, which was different from previously reported observations that the tonsil was the most frequent false negative location (*16*). Recently, Serfling et al (*26*) reported ^{68}Ga-FAPI-PET/CT showed a better visual detection of the malignant primary in Waldeyer's tonsillar ring than ^{18}F-FDG-PET/CT. However, the representative cases could provide positive findings of primary site by ^{18}F-FDG-PET/CT alone in terms of HNCUP. Another previous research demonstrated that an SUV_{max} ratio of FDG uptake between tonsils of ≥ 1.6 could be regarded as malignancy and used to guide biopsy (*28*). In this study, two patients were diagnosed with palatine tonsil carcinoma by tonsillectomy. Puzzlingly, ^{18}F-FDG-PET/CT revealed no visual difference between right and left palatine tonsils in both two cases. Furthermore, the SUV_{max} ratios of FDG uptake were all approximate equivalent to 1.00 (1.07 and 1.04 for patient 2 and 3, respectively), which was mistaken as physiologic uptake. By contrast, ^{68}Ga-FAPI-PET/CT showed intensive uptake in tumor site and low uptake in the normal site, resulting in an obvious visual difference (SUV_{max} ratio = 3.46 and 8.21, respectively). In line with our results, Syed et al (*25*) demonstrated high FAPI avidity within tumorous lesions and low background

uptake in healthy tissues of the head and neck region. In other ways, this study once again emphases the potential role of ^{68}Ga-FAPI-PET/CT in detecting palatine tonsil carcinoma, particularly in FDG-negative patients.

In addition to high grade physiologic uptake of head and neck, small size of the lesions was the major reason for the false negative FDG findings due to the partial volume effect and low tumor glucose metabolic activity (*29,30*). In this study, ^{18}F-FDG-PET/CT missed 3 of 7 primary tumors by reason of the small size (diameter < 10 mm). Encouragingly, ^{68}Ga-FAPI-PET/CT revealed moderate uptake (SUV_{max} = 2.60, 3.20, and 3.60 for patient 1, 6, and 7, respectively) and clearly visual difference (SUV_{max} ratio = 2.17, 2.91, and 3.27, respectively) in these primary tumors with small size, which was consistent with previous research (*24*). The uptake of FAPI is mainly based on the expression of FAP on CAFs among solid tumor microenvironment. And even small primary tumors of T1 stage could show a moderate FAP expression (*26*). Thus, ^{68}Ga-FAPI could serve as an alternative tracer for identifying primary tumor of small size to reduce the false negative results by ^{18}F-FDG-PET/CT.

Most of the researches focus on SCC, as it is the most frequent pathological type of HNCUP (*3-5*). However, some other pathological types, like adenocarcinoma and neuroendocrine carcinoma, may cause diagnostic difficulties in clinical practice due to inexperience. Moreover, when it comes to cervical metastatic adenocarcinoma, diagnostic resection of salivary gland is not recommended even after thorough non-invasive investigations. Furthermore, salivary gland cancers show paucity of FDG avidity (*31*), which was proofed again in our study (patient 4 and 5). Some non-FDG radiopharmaceuticals, e.g., ^{18}F-Fluorothymidine, ^{68}Ga -DOTA-Somatostatin Analogs, and ^{18}F-Fluoromisonidazole, are recommended to detect primary tumor of HNCUP (*32*). However, these tracers are too specific to identify all types of head and neck cancers. Promisingly, recent studies have demonstrated ^{68}Ga-FAPI can evaluate a broad spectrum of malignancies, including adenocarcinoma, neuroendocrine carcinoma, and well-

differentiated carcinoma and so on (*23,24*). In this study, ^{68}Ga-FAPI showed intensive uptake in submandibular gland (SUV_{max} = 16.50 and 15.80, respectively), providing sufficient information for following surgery. Notably, ^{68}Ga-FAPI had a higher detection rate in adenocarcinoma (2/2, 100%) than SCC (5/16, 31.25%) of HNCUP, which indicated ^{68}Ga-FAPI was more sensitive to adenocarcinoma. However, further research with larger sample size is needed to verify this result.

With regard to the detection of regional and distant metastases, the performance of ^{68}Ga-FAPI-PET/CT varies among different researches (*24,26*). In our study, ^{68}Ga-FAPI-PET/CT showed similar performance ($p > 0.05$) with ^{18}F-FDG-PET/CT in detecting both lymph node and bone metastases. Considering that radiation therapy is one of the most important modalities of treating HNCUP, the advantages of ^{68}Ga-FAPI-PET/CT in both primary tumors and metastases may play a vital role in gross tumor volume delineation.

There are some limitations in this study. First, the main limitation is the relatively small number of patients, and the number of pathologic types is uneven. In the future, larger population cohort studies with more cancer types need to take into account. Second, immunohistochemistry for FAP expression of primary tumors and metastases is lacking. Hence, FAPI imaging and FAP expression control studies are also necessary in the future.

CONCLUSION

This study demonstrated that ^{68}Ga-FAPI-PET/CT can improve the detection rate of primary tumor in HNCUP patients with negative FDG findings. Furthermore, with regard to the evaluation of metastatic lesions, ^{68}Ga-FAPI-PET/CT showed similar performance with ^{18}F-FDG PET/CT. Since HNCUP is in need of improved detection rate, future

research containing more patients with HNCUP should be considered to evaluate the clinical value of ^{68}Ga-FAPI-PET/CT in these patients.

DISCLOSURE

This work was funded by National Natural Science Foundation of China (Grant number 81771861, 81971648, and 81901778) and Shanghai Anticancer Association Program (Grant number HYXH2021004). No other potential conflict of interest relevant to this article was reported.

ACKNOWLEDGEMENT

We would like to thank the multidisciplinary team of head and neck cancer in our center for the great help to our work.

KEY POINTS

QUESTION: Does ^{68}Ga-FAPI-PET/CT have value for identifying primary tumor in FDG-negative patients with head and neck cancer of unknown primary (HNCUP)?

PERTINET FINDINGS: In this prospective study, ^{68}Ga-FAPI-PET/CT improved the detection rate (38.89%) of primary tumor in HNCUP patients with negative FDG findings.

IMPLICATIONS FOR PATIENT CARE: Our study provides a new strategy for identifying primary tumor in patients with HNCUP, which may change their treatment decisions.

REFERENCES

1. Kennel T, Garrel R, Costes V, Boisselier P, Crampette L, Favier V. Head and neck carcinoma of unknown primary. *Eur Ann Otorhinolaryngol Head Neck Dis.* 2019;136:185-192.

2. Pfister DG, Spencer S, Adelstein D, et al. Head and neck cancers, version 2.2020, NCCN clinical practice guidelines in oncology. *J Natl Compr Canc Netw.* 2020;18:873-898.

3. Maghami E, Ismaila N, Alvarez A, et al. Diagnosis and management of squamous cell carcinoma of unknown primary in the head and neck: ASCO guideline. *J Clin Oncol.* 2020;38:2570-2596.

4. Galloway TJ, Ridge JA. Management of squamous cancer metastatic to cervical nodes with an unknown primary site. *J Clin Oncol.* 2015;33:3328-3337.

5. Moy J, Li R. Approach to the patient with unknown primary squamous cell carcinoma of the head and neck. *Curr Treat Options Oncol.* 2020;21:93.

6. Keller LM, Galloway TJ, Holdbrook T, et al. p16 status, pathologic and clinical characteristics, biomolecular signature, and long-term outcomes in head and neck squamous cell carcinomas of unknown primary. *Head Neck.* 2014;36:1677-1684.

7. Golusinski P, Di Maio P, Pehlivan B, et al. Evidence for the approach to the diagnostic evaluation of squamous cell carcinoma occult primary tumors of the head and neck. *Oral Oncol.* 2019;88:145-152.

8. Arosio AD, Pignataro L, Gaini RM, Garavello W. Neck lymph node metastases from unknown primary. *Cancer Treat Rev.* 2017;53:1-9.

9. Junn JC, Soderlund KA, Glastonbury CM. Imaging of head and neck cancer with CT, MRI, and US. *Semin Nucl Med.* 2021;51:3-12.

10. Regelink G, Brouwer J, de Bree R, et al. Detection of unknown primary tumours and distant metastases in patients with cervical metastases: value of FDG-PET versus conventional modalities. *Eur J Nucl Med Mol Imaging.* 2002;29:1024-1030.

11. Freudenberg LS, Fischer M, Antoch G, et al. Dual modality of (18)F-fluorodeoxyglucose-positron emission tomography/computed tomography in patients with cervical carcinoma of unknown primary. *Med Princ Pract.* 2005;14:155-160.

12. Waltonen JD, Ozer E, Hall NC, Schuller DE, Agrawal A. Metastatic carcinoma of the neck of unknown primary origin: evolution and efficacy of the modern workup. *Arch Otolaryngol Head Neck Surg.* 2009;135:1024-1029.

13. Rusthoven KE, Koshy M, Paulino AC. The role of fluorodeoxyglucose positron emission tomography in cervical

lymph node metastases from an unknown primary tumor. *Cancer.* 2004;101:2641-2649.

14. Zhu L, Wang N. (18)F-fluorodeoxyglucose positron emission tomography-computed tomography as a diagnostic tool in patients with cervical nodal metastases of unknown primary site: a meta-analysis. *Surg Oncol.* 2013;22:190-194.

15. Lee JR, Kim JS, Roh JL, et al. Detection of occult primary tumors in patients with cervical metastases of unknown primary tumors: comparison of (18)F-FDG PET/CT with contrast-enhanced CT or CT/MR imaging-prospective study. *Radiology.* 2015;274:764-771.

16. Liu Y. FDG PET/CT for metastatic squamous cell carcinoma of unknown primary of the head and neck. *Oral Oncol.* 2019;92:46-51.

17. Goel R, Moore W, Sumer B, Khan S, Sher D, Subramaniam RM. Clinical practice in PET/CT for the management of head and neck squamous cell cancer. *AJR Am J Roentgenol.* 2017;209:289-303.

18. Szyszko TA, Cook GJR. PET/CT and PET/MRI in head and neck malignancy. *Clin Radiol.* 2018;73:60-69.

19. Kuzet SE, Gaggioli C. Fibroblast activation in cancer: when seed fertilizes soil. *Cell Tissue Res.* 2016;365:607-619.

20. Koczorowska MM, Tholen S, Bucher F, et al. Fibroblast activation protein-alpha, a stromal cell surface protease, shapes key features of cancer associated fibroblasts through proteome and degradome alterations. *Mol Oncol.* 2016;10:40-58.

21. Rettig WJ, Garin-Chesa P, Beresford HR, Oettgen HF, Melamed MR, Old LJ. Cell-surface glycoproteins of human sarcomas: differential expression in normal and malignant tissues and cultured cells. *Proc Natl Acad Sci U S A.* 1988;85:3110-3114.

22. Scanlan MJ, Raj BK, Calvo B, et al. Molecular cloning of fibroblast activation protein alpha, a member of the serine protease family selectively expressed in stromal fibroblasts of epithelial cancers. *Proc Natl Acad Sci U S A.* 1994;91:5657-5661.

23. Kratochwil C, Flechsig P, Lindner T, et al. (68)Ga-FAPI PET/CT: tracer uptake in 28 different kinds of cancer. *J Nucl Med.* 2019;60:801-805.

24. Chen H, Pang Y, Wu J, et al. Comparison of [(68)Ga]Ga-DOTA-FAPI-04 and [(18)F] FDG PET/CT for the diagnosis of primary and metastatic lesions in patients with various types of cancer. *Eur J Nucl Med Mol Imaging.* 2020;47:1820-1832.

25. Syed M, Flechsig P, Liermann J, et al. Fibroblast activation protein inhibitor (FAPI) PET for diagnostics and

advanced targeted radiotherapy in head and neck cancers. *Eur J Nucl Med Mol Imaging.* 2020;47:2836-2845.

26. Serfling S, Zhi Y, Schirbel A, et al. Improved cancer detection in Waldeyer's tonsillar ring by (68)Ga-FAPI PET/CT imaging. *Eur J Nucl Med Mol Imaging.* 2021;48:1178-1187.

27. Lindner T, Loktev A, Altmann A, et al. Development of quinoline-based theranostic ligands for the targeting of fibroblast activation protein. *J Nucl Med.* 2018;59:1415-1422.

28. Pencharz D, Dunn J, Connor S, et al. Palatine tonsil SUVmax on FDG PET-CT as a discriminator between benign and malignant tonsils in patients with and without head and neck squamous cell carcinoma of unknown primary. *Clin Radiol.* 2019;74:165.e117-165.e123.

29. Redondo-Cerezo E, Martinez-Cara JG, Jimenez-Rosales R, et al. Endoscopic ultrasound in gastric cancer staging before and after neoadjuvant chemotherapy. A comparison with PET-CT in a clinical series. *United European Gastroenterol J.* 2017;5:641-647.

30. Spadafora M, Pace L, Evangelista L, et al. Risk-related (18)F-FDG PET/CT and new diagnostic strategies in patients with solitary pulmonary nodule: the ITALIAN multicenter trial. *Eur J Nucl Med Mol Imaging.* 2018;45:1908-1914.

31. Wong WL. PET-CT for staging and detection of recurrence of head and neck cancer. *Semin Nucl Med.* 2021;51:13-25.

32. Eisenmenger LB. Non-FDG radiopharmaceuticals in head and neck PET imaging: current techniques and future directions. *Semin Ultrasound CT MR.* 2019;40:424-433.

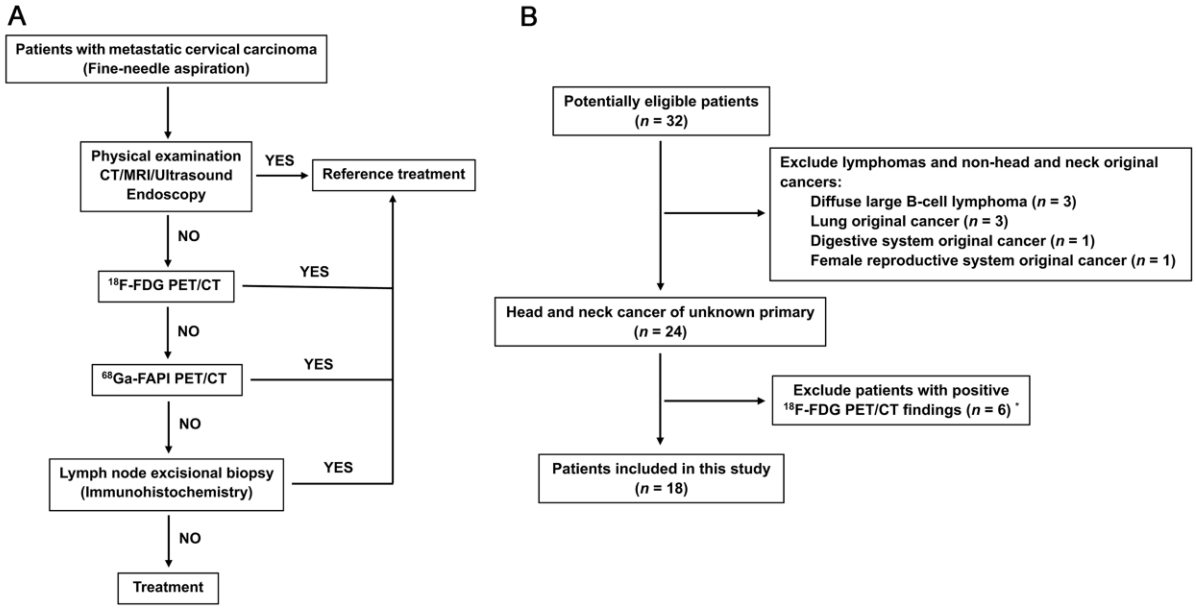

FIGURE 1. Flowchart of diagnostic workup (A) and patient selection (B). "YES" means the primary tumor was identified by these techniques and further confirmed by pathology, and "NO" indicates these techniques couldn't identify the primary tumor. * ^{68}Ga-FAPI-PET/CT could also identify the primary tumor in these patients.

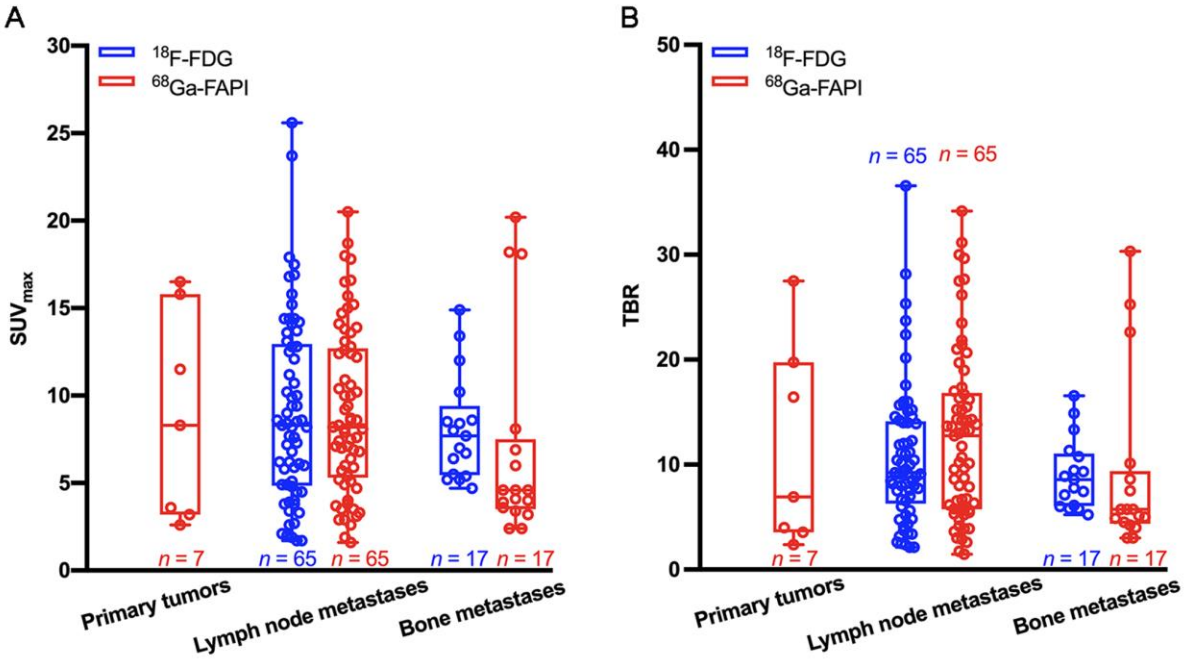

FIGURE 2. Boxplots of SUV_{max} (A) and TBR (B) on ^{18}F-FDG versus ^{68}Ga-FAPI-PET/CT.

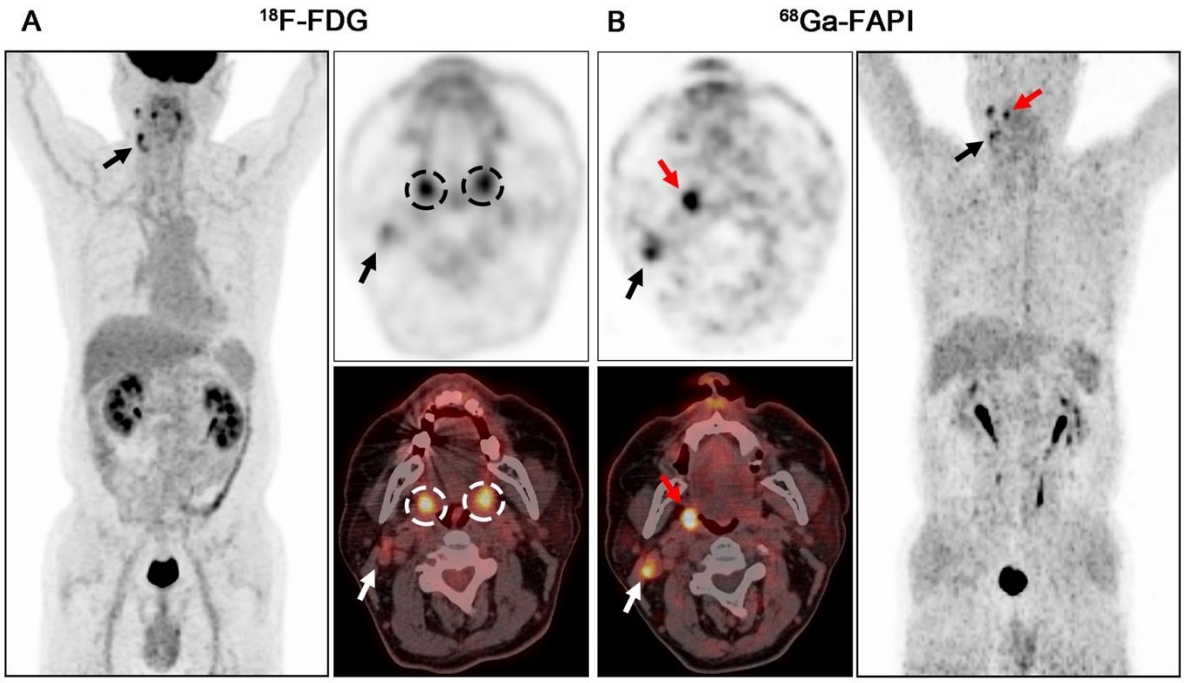

FIGURE 3. PET/CT scans with the ^{18}F-FDG (A) and ^{68}Ga-FAPI (B) in a 63-year-old male patient (patient 2) with metastatic squamous cell carcinoma (SCC) of the right neck. ^{18}F-FDG-PET/CT was negative for the detection of the primary. The increased uptake of FDG was detected in palatine tonsils of both right and left sides (A, black and white dashed circles; SUV_{max} = 6.40 and 6.00, respectively), resulting an SUV_{max} ratio of 1.07. On ^{68}Ga-FAPI-PET/CT, there was asymmetric fullness with intensive uptake in the right palatine tonsil (B, red arrow; SUV_{max} = 8.30), while low background uptake was seen in the left palatine tonsil (SUV_{max} ratio = 3.46). Subsequent tonsillectomy confirmed SCC. Black and white arrows indicate the metastatic lymph nodes.

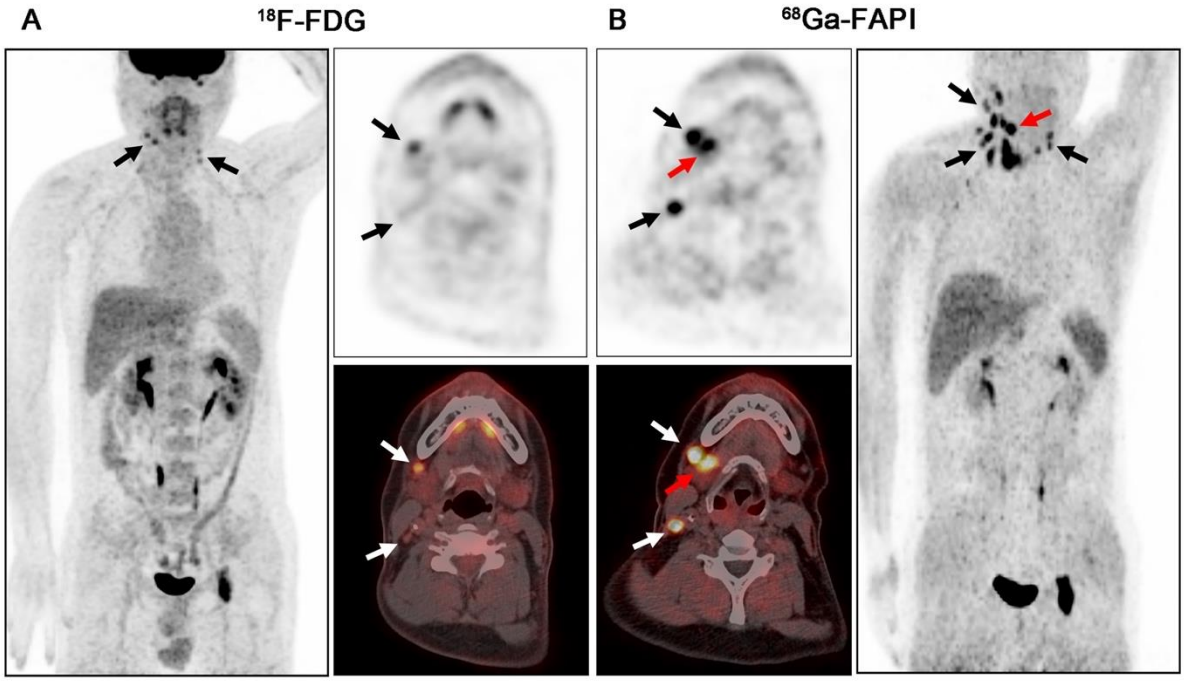

FIGURE 4. PET/CT scans with the ^{18}F-FDG (A) and ^{68}Ga-FAPI (B) in a 41-year-old male patient (patient 5) with metastatic adenocarcinoma of the right neck. ^{18}F-FDG-PET/CT was negative for the detection of the primary. On ^{68}Ga-FAPI-PET/CT, there was an intensive uptake in the right submandibular gland (B, red arrow; SUV_{max} = 15.80), while low background uptake was seen in the left submandibular gland (SUV_{max} ratio = 6.87). Subsequent surgery confirmed salivary ductal carcinoma. Black and white arrows indicate the metastatic lymph nodes.

TABLE 1. Patients' characteristics

Patient No.	Gender	Age (years)	EBV-DNA status	HPV status	p16 status	Pathologic type of cervical lymph node
1	M	52	P	U	U	SCC
2	M	63	N	P	P	SCC
3	M	58	N	P	P	SCC
4	M	50	N	U	U	AC
5	M	41	U	P	P	AC
6	M	55	N	U	U	SCC
7	M	54	N	N	N	SCC
8	M	72	N	U	U	SCC
9	M	61	N	P	N	SCC
10	M	47	N	N	P	SCC
11	M	62	N	N	N	SCC
12	F	55	P	N	N	SCC
13	M	63	N	U	U	SCC
14	F	67	N	U	U	SCC
15	M	40	N	P	P	SCC
16	M	24	N	N	N	SCC
17	M	55	N	U	U	SCC
18	M	51	U	P	P	SCC

EBV-DNA = Epstein-Barr virus deoxyribonucleic acid; HPV = human papillomavirus; M = male; F = female; P = positive; N = negative; U = unknown; SCC = squamous cell carcinoma; AC = adenocarcinoma

TABLE 2. Comparison of metastatic lesions on ^{18}F-FDG and ^{68}Ga-FAPI-PET/CT in eighteen patients with HNCUP

Patient No.	Metastases		Range of metastases size (mm)	^{18}F-FDG		^{68}Ga-FAPI		*p*-value	
	Location	No.		SUV_{max}	TBR	SUV_{max}	TBR	SUV_{max}	TBR
1	LN	3	7 - 8	5.27 ± 1.29	4.39 ± 1.07	2.27 ± 0.91	2.06 ± 0.82		
2	LN	2	7 - 20	6.55 ± 0.92	7.28 ± 1.02	7.10 ± 0.42	5.92 ± 0.35		
3	LN	2	10 - 16	8.10 ± 1.84	9.00 ± 2.04	14.40 ± 0.85	20.57 ± 1.21		
4	LN	16	7 - 22	10.78 ± 3.13	11.98 ± 3.48	13.69 ± 4.19	22.81 ± 6.98		
	Bone	1	N/A	8.00	8.89	18.20	30.33		
5	LN	8	4 - 8	2.70 ± 1.07	3.38 ± 1.33	9.41 ± 2.40	11.77 ± 3.00		
	Bone	1	N/A	8.60	10.75	20.20	25.25		
6	LN	2	17 - 22	5.60 ± 4.24	8.00 ± 6.06	5.35 ± 0.92	5.94 ± 1.02		
7	LN	1	17	7.60	8.44	12.80	14.22		
8	LN	1	38	25.60	36.57	15.20	19.00		
9	LN	4	7 - 17	15.78 ± 1.61	13.15 ± 1.34	3.83 ± 1.32	4.25 ± 1.47		
10	LN	1	27	7.30	9.13	3.10	2.58		
11	LN	2	13 - 20	15.35 ± 3.61	19.19 ± 4.51	5.60 ± 2.69	8.00 ± 3.84		
12	LN	3	13 - 21	10.80 ± 5.17	18.00 ± 8.62	5.63 ± 3.82	8.05 ± 5.46		
13	LN	1	10	6.20	8.86	8.60	9.56		
14	LN	8	5 - 11	6.81 ± 4.30	11.35 ± 7.17	7.60 ± 3.31	8.44 ± 3.68		
15	LN	1	5	2.10	2.63	2.90	3.63		
16	LN	3	12 - 26	12.63 ± 2.29	14.04 ± 2.55	11.87 ± 3.27	14.83 ± 4.08		
	Bone	15	N/A	8.08 ± 3.19	8.98 ± 3.55	5.33 ± 3.86	6.66 ± 4.83		
17	LN	3	10 - 19	8.80 ± 1.28	8.00 ± 1.16	7.60 ± 0.50	15.20 ± 1.00		
18	LN	4	4 - 18	11.08 ± 9.02	11.08 ± 9.02	7.58 ± 3.51	9.47 ± 4.39		
Sum	LN	65	4 - 26	9.05 ± 5.29	10.65 ± 6.59	9.08 ± 4.69	12.80 ± 8.11	0.975	0.100
	Bone	17	N/A	8.11 ± 3.00	9.08 ± 3.35	6.96 ± 5.87	9.14 ± 8.40	0.478	0.976

PET semiquantitative parameters were presented as means with standard deviation; HNCUP = head and neck cancer of unknown primary; TBR = tumor-to-background ratio; LN = lymph node; N/A = not applicable

TABLE 3. Primary tumor characteristics and semiquantitative parameters of ^{68}Ga-FAPI-PET/CT

Patient No.	TNM	Primary tumor location	Pathologic type	Tumor size (mm)	^{68}Ga-FAPI		
					SUV_{max}	TBR	SUV_{max} ratio
1	T1N1M0 Stage II	Nasopharynx top wall	NDSCC	6 × 5	2.60	2.36	2.17
2	T1N1M0 Stage I	Palatine tonsil right side	SCC	11 × 10	8.30	6.92	3.46
3	T1N1M0 Stage I	Palatine tonsil right side	SCC	13 × 10	11.50	16.43	8.21
4	T2N2M1 Stage IVC	Submandibular gland right side	SDC	23 × 20	16.50	27.50	4.58
5	T1N2M1 Stage IVC	Submandibular gland right side	SDC	17 × 13	15.80	19.75	6.87
6	T1N1M0 Stage III	Hypopharynx posterior wall	SCC	5 × 3	3.20	3.56	2.91
7	T1N1M0 Stage III	Sinus piriformis right side	SCC	6 × 5	3.60	4.00	3.27

TBR = tumor-to-background ratio; NDSCC = non-keratinizing differentiated squamous cell carcinomas; SCC = squamous cell carcinoma; SDC = salivary ductal carcinoma

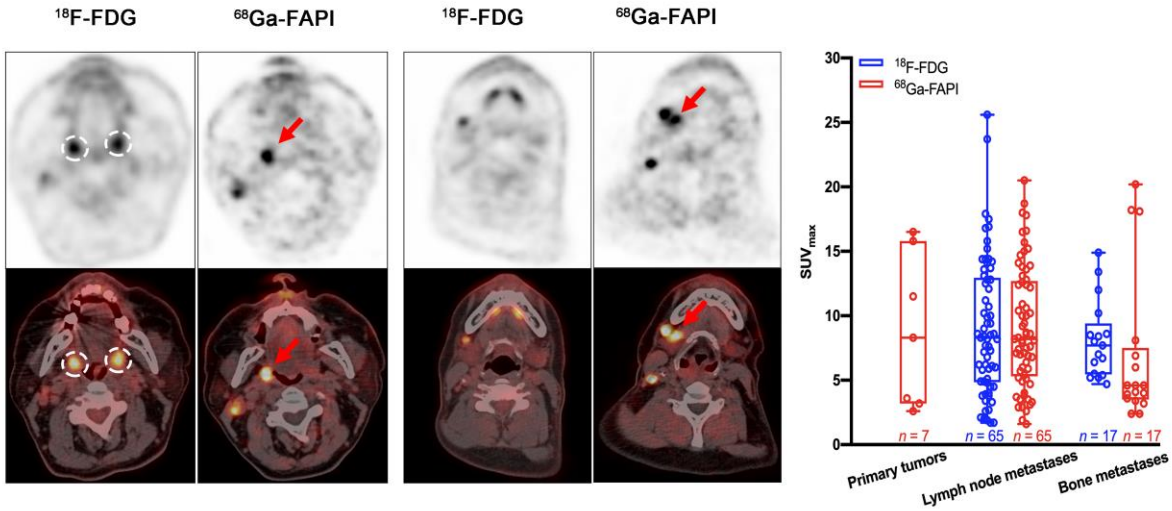

Graphic Abstract. ^{68}Ga-FAPI-PET/CT can improve the detection rate of primary tumor in head and neck cancer of unknown primary patients with negative FDG findings, and show similar performance with ^{18}F-FDG-PET/CT in assessing metastases.

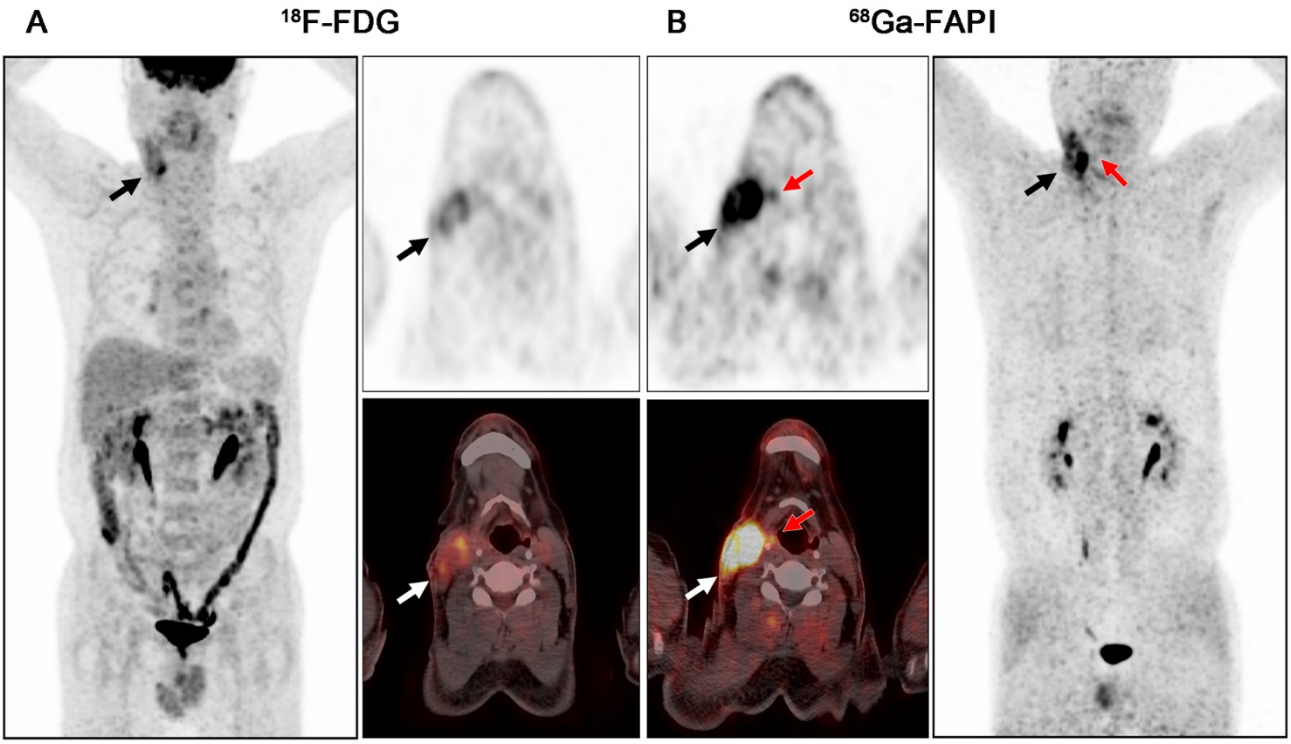

SUPPLEMENTAL FIGURE 1. PET/CT scans with the ^{18}F-FDG (A) and ^{68}Ga-FAPI (B) in a 54-year-old male patient (patient 7) with metastatic squamous cell carcinoma (SCC) of the right neck. ^{18}F-FDG-PET/CT was negative for the detection of the primary. On ^{68}Ga-FAPI-PET/CT, there was a moderate uptake in the right sinus piriformis (B, red arrow; SUV_{max} = 3.60), while low background uptake was seen in the left sinus piriformis (SUV_{max} ratio = 3.27). Subsequent biopsy confirmed SCC. Black and white arrows indicate the metastatic lymph node.

SUPPLEMENTAL TABLE 1. Detailed information of primary and metastatic lesions on ^{18}F-FDG and ^{68}Ga-FAPI-PET/CT in eighteen patients

Patients No.	Lesion	Location	^{18}F-FDG			^{68}Ga-FAPI		
			$tSUV_{max}$	$bSUV_{mean}$	TBR	$tSUV_{max}$	$bSUV_{mean}$	TBR
1	Primary tumor	Nasopharynx top wall	-	-	-	2.60	1.10	2.36
	Lymph node	Neck level II B	6.20	1.20	5.17	3.30	1.10	3.00
	Lymph node	Neck level II A	5.80	1.20	4.83	1.90	1.10	1.73
	Lymph node	Neck level V A	3.80	1.20	3.17	1.60	1.10	1.45
2	Primary tumor	Right palatine tonsil	-	-	-	8.30	1.20	6.92
	Lymph node	Neck level II B	5.90	0.90	6.56	6.80	1.20	5.67
	Lymph node	Neck level II A	7.20	0.90	8.00	7.40	1.20	6.17
3	Primary tumor	Right palatine tonsil	-	-	-	11.50	0.70	16.43
	Lymph node	Neck level II B	9.40	0.90	10.44	15.00	0.70	21.43
	Lymph node	Neck level II B	6.80	0.90	7.56	13.80	0.70	19.71
4	Primary tumor	Right submandibular gland	-	-	-	16.50	0.60	27.50
	Lymph node	Neck level II B	9.90	0.90	11.00	14.10	0.60	23.50
	Lymph node	Neck level II B	15.80	0.90	17.56	18.70	0.60	31.17
	Lymph node	Neck level II B	10.70	0.90	11.89	12.40	0.60	20.67
	Lymph node	Neck level II A	13.60	0.90	15.11	10.00	0.60	16.67
	Lymph node	Neck level I B	3.90	0.90	4.33	8.60	0.60	14.33
	Lymph node	Neck level III	8.20	0.90	9.11	8.30	0.60	13.83
	Lymph node	Neck level IV	8.60	0.90	9.56	7.90	0.60	13.17
	Lymph node	Chest level 1 R	12.50	0.90	13.89	13.10	0.60	21.83
	Lymph node	Chest level 1 L	8.30	0.90	9.22	8.20	0.60	13.67
	Lymph node	Chest level 2 R	12.80	0.90	14.22	15.70	0.60	26.17
	Lymph node	Chest level 4 R	13.10	0.90	14.56	20.50	0.60	34.17
	Lymph node	Chest level 5	14.40	0.90	16.00	16.60	0.60	27.67
	Lymph node	Chest level 6	8.20	0.90	9.11	12.60	0.60	21.00
	Lymph node	Chest level 7	9.00	0.90	10.00	16.50	0.60	27.50
	Lymph node	Chest level 10 R	14.10	0.90	15.67	17.80	0.60	29.67
	Lymph node	Chest level 10 L	9.40	0.90	10.44	18.00	0.60	30.00
	Bone	Fifth cervical vertebra	8.00	0.90	8.89	18.20	0.60	30.33
5	Primary tumor	Right submandibular gland	-	-	-	15.80	0.80	19.75
	Lymph node	Neck level II B	1.90	0.80	2.38	12.40	0.80	15.50
	Lymph node	Neck level II A	1.70	0.80	2.13	9.40	0.80	11.75

	Lymph node	Neck level I B	4.50	0.80	5.63	10.40	0.80	13.00
	Lymph node	Neck level III	1.70	0.80	2.13	12.20	0.80	15.25
	Lymph node	Neck level III	2.00	0.80	2.50	6.90	0.80	8.63
	Lymph node	Neck level III	3.80	0.80	4.75	7.00	0.80	8.75
	Lymph node	Neck level IV	3.30	0.80	4.13	10.60	0.80	13.25
	Lymph node	Neck level IV	2.70	0.80	3.38	6.40	0.80	8.00
	Bone	Acetabulum	8.60	0.80	10.75	20.20	0.80	25.25
6	Primary tumor	Hypopharynx posterior wall	-	-	-	3.20	0.90	3.56
	Lymph node	Neck level II A	2.60	0.70	3.71	4.70	0.90	5.22
	Lymph node	Neck level III	8.60	0.70	12.29	6.00	0.90	6.67
7	Primary tumor	Right sinus piriformis	-	-	-	3.60	0.90	4.00
	Lymph node	Neck level III	7.60	0.90	8.44	12.80	0.90	14.22
8	Lymph node	Neck level III	25.60	0.70	36.57	15.20	0.80	19.00
9	Lymph node	Neck level II B	16.80	1.20	14.00	2.60	0.90	2.89
	Lymph node	Neck level V A	17.50	1.20	14.58	5.70	0.90	6.33
	Lymph node	Neck level II A	14.40	1.20	12.00	3.50	0.90	3.89
	Lymph node	Neck level III	14.40	1.20	12.00	3.50	0.90	3.89
10	Lymph node	Neck level II A	7.30	0.80	9.13	3.10	1.20	2.58
11	Lymph node	Neck level II A	17.90	0.80	22.38	7.50	0.70	10.71
	Lymph node	Neck level III	12.80	0.80	16.00	3.70	0.70	5.29
12	Lymph node	Neck level II B	5.10	0.60	8.50	10.00	0.70	14.29
	Lymph node	Neck level II B	15.20	0.60	25.33	2.90	0.70	4.14
	Lymph node	Neck level II A	12.10	0.60	20.17	4.00	0.70	5.71
13	Lymph node	Neck level I B	6.20	0.70	8.86	8.60	0.90	9.56
14	Lymph node	Neck level II B	8.40	0.60	14.00	9.20	0.90	10.22
	Lymph node	Neck level II B	16.90	0.60	28.17	14.70	0.90	16.33
	Lymph node	Neck level III	6.10	0.60	10.17	8.70	0.90	9.67
	Lymph node	Left axillary	4.50	0.60	7.50	5.10	0.90	5.67
	Lymph node	Left axillary	4.90	0.60	8.17	7.10	0.90	7.89
	Lymph node	Left axillary	4.90	0.60	8.17	5.90	0.90	6.56
	Lymph node	Left axillary	4.00	0.60	6.67	4.90	0.90	5.44
	Lymph node	Left axillary	4.80	0.60	8.00	5.20	0.90	5.78
15	Lymph node	Neck level II A	2.10	0.80	2.63	2.90	0.80	3.63
16	Lymph node	Neck level II B	14.20	0.90	15.78	8.10	0.80	10.13
	Lymph node	Neck level II B	13.70	0.90	15.22	13.90	0.80	17.38

	Lymph node	Neck level II B	10.00	0.90	11.11	13.60	0.80	17.00
	Bone	Atlas	7.70	0.90	8.56	4.60	0.80	5.75
	Bone	Sixth cervical vertebra	6.40	0.90	7.11	4.60	0.80	5.75
	Bone	Seventh cervical vertebra	5.20	0.90	5.78	4.10	0.80	5.13
	Bone	Second thoracic vertebra	8.50	0.90	9.44	3.60	0.80	4.50
	Bone	Twelfth thoracic vertebra	6.70	0.90	7.44	4.00	0.80	5.00
	Bone	Second lumbar vertebra	8.40	0.90	9.33	8.10	0.80	10.13
	Bone	Sacrum	14.90	0.90	16.56	18.10	0.80	22.63
	Bone	Right ilium	13.40	0.90	14.89	6.00	0.80	7.50
	Bone	Left ilium	12.00	0.90	13.33	3.90	0.80	4.88
	Bone	Right pubis	10.20	0.90	11.33	4.60	0.80	5.75
	Bone	Left scapula	5.20	0.90	5.78	3.40	0.80	4.25
	Bone	Right scapula	4.70	0.90	5.22	2.40	0.80	3.00
	Bone	Left ninth rib	5.40	0.90	6.00	3.20	0.80	4.00
	Bone	Right eighth rib	7.00	0.90	7.78	6.90	0.80	8.63
	Bone	Right femur	5.50	0.90	6.11	2.40	0.80	3.00
17	Lymph node	Neck level II B	10.20	1.10	9.27	8.10	0.50	16.20
	Lymph node	Neck level II A	8.50	1.10	7.73	7.60	0.50	15.20
	Lymph node	Neck level II A	7.70	1.10	7.00	7.10	0.50	14.20
18	Lymph node	Neck level II B	23.70	1.00	23.70	10.90	0.80	13.63
	Lymph node	Neck level II A	11.20	1.00	11.20	10.20	0.80	12.75
	Lymph node	Neck level II A	6.00	1.00	6.00	5.40	0.80	6.75
	Lymph node	Neck level II B	3.40	1.00	3.40	3.80	0.80	4.75

$tSUV_{max}$ = the maximum SUV of tumor lesion; $bSUV_{mean}$ = the mean SUV of muscle; TBR = tumor-to-background ratio